

Supplemental Materials

Molecular Biology of the Cell

Postema et al.

SUPPLEMENTAL INFORMATION

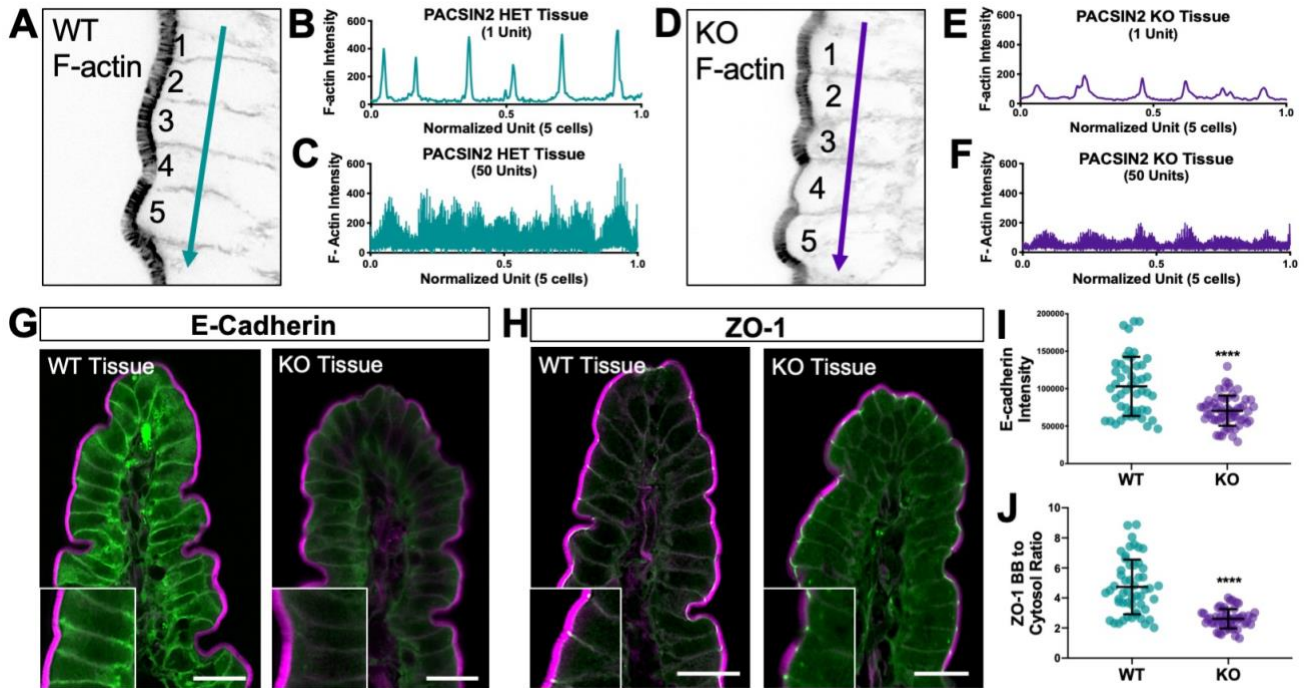
PACSIN2-dependent apical endocytosis regulates the morphology of epithelial microvilli

Meagan M. Postema, Nathan E. Grega-Larson, Leslie M. Meenderink, and Matthew J. Tyska

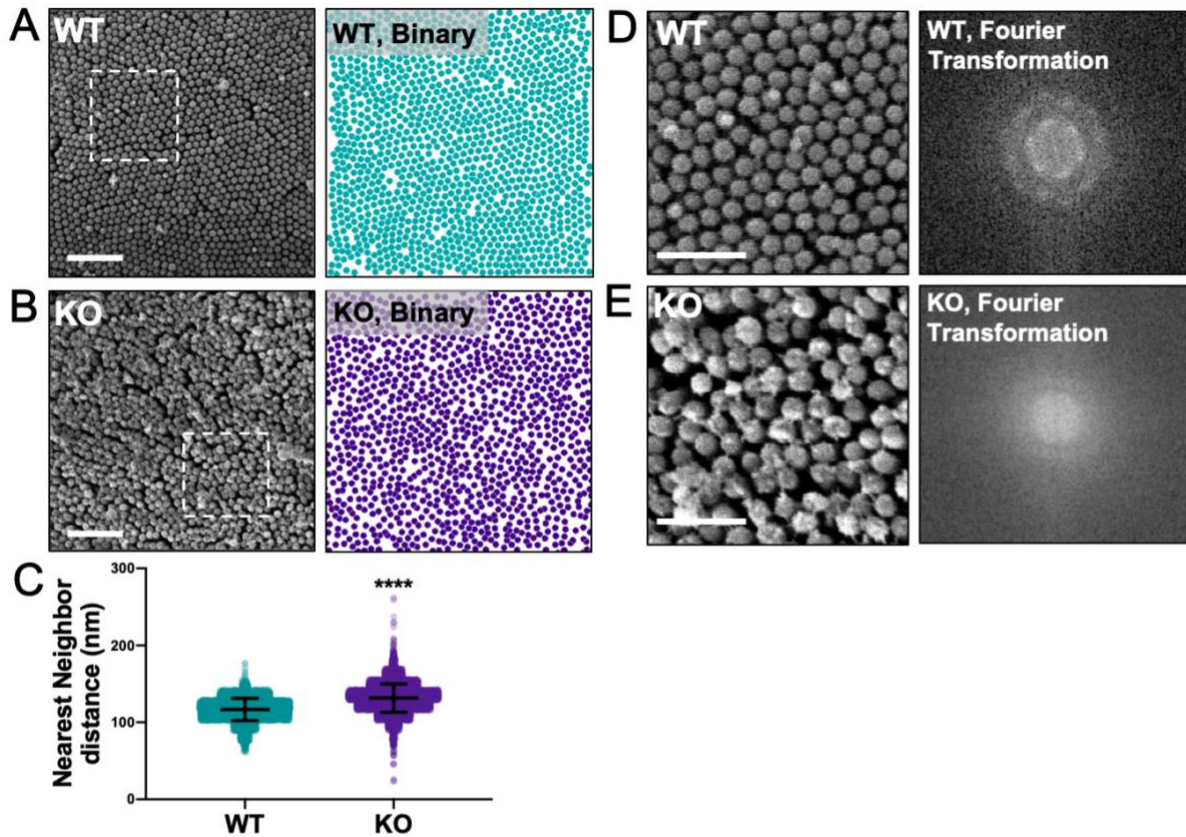
CONTAINS:

Supplemental Figures 1-3

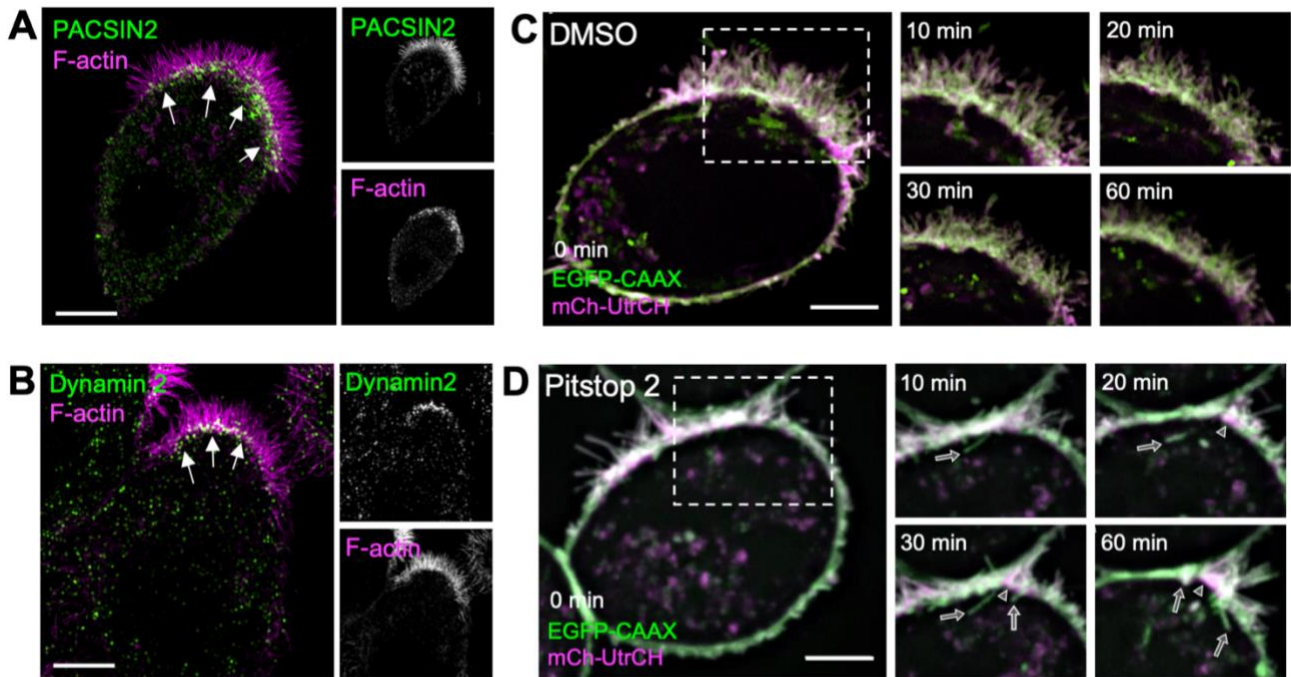
Supplemental Figure Legends



Supplemental Figure 1, Related to Figure 2. Loss of PACSIN2 leads to junctional instability. (A, D) Representative images used in quantification in D, E, G, H; phalloidin stained. **(B, C)** Top, raw intensity data of a line (depicted by teal arrow in C) through 5 total cells in WT tissue, peaks indicate the actin junctional intensity. Bottom, raw intensity data of lines through 5 cells in 50 WT tissue sections, lines have been smoothed for ease of viewing. **(E, F)** Top, raw intensity data of a line (depicted by purple arrow in F) through 5 cells in PACSIN2 KO tissue, peaks indicate the actin junctional intensity. Bottom, raw intensity data of lines through 5 total cells in 50 KO tissue sections, lines have been smoothed for ease of viewing. **(G)** Endogenous E-Cadherin (green) and phalloidin (F-actin, magenta) labelling of WT and PACSIN2 KO frozen tissue sections. Scale bars, 20 μ m. **(H)** Endogenous ZO-1 (green) and phalloidin (F-actin, magenta) labelling of WT and PACSIN2 KO frozen tissue sections. Scale bars, 20 μ m. **(I)** Quantification of E-Cadherin signal intensity between WT (n = 47 measurements) and PACSIN2 KO (n = 60 measurements). **(J)** Quantification of the ratio of ZO-1 BB to cytosol ratio between WT (n = 52 measurements) and PACSIN2 KO (n = 50 measurements). Error bars indicate \pm SD; p value was calculated using a t test (****p<0.0001).



Supplemental Figure 2, Related to Figure 4. Microvillar packing is decreased in the PACSIN2 KO mouse. (A, B) SEM images WT (A) and KO (B) brush borders reveal microvillar packing defects in KO samples. Binary images indicating microvilli were used to determine the nearest neighbor distances. **(C)** Quantification of the nearest neighbor distance from mask. The mean center to center distance between microvilli was calculated; 6 fields of microvilli per condition. Error bars indicate \pm SD; p value was calculated using a t test (**** $p < 0.0001$). **(D, E)** $1.5 \mu\text{m}^2$ images showing differences in microvillar packing and the abnormal Fourier transformation obtained in the KO sample.



Supplemental Figure 3, Related to Figure 5. Pitstop2 inhibits endocytosis in W4 cells. (A) SIM projection of a W4 cell showing endogenous PACSIN2 (green) and stained with phalloidin (magenta). Arrows point to PACSIN2 puncta at the base of the brush border. **(B)** SIM projection of a W4 cell showing endogenous Dynamin2 (green) and stained with phalloidin (magenta). Arrows point to Dynamin2 puncta at the base of the brush border. **(C, D)** Montages of DMSO control and 30 μ M Pitstop 2 treated W4 cell expressing EGFP-CAAX box (membrane, green) and mCherry-UtrCH (F-actin, magenta). Arrows in Pitstop 2 cell (D) indicate membrane tubules forming into the cytosol, arrowheads indicate membrane lifting. Scale bars, 5 μ m.